CivilEng

MDPI

Article

Effects of Marble Particle Size and Gamma Irradiation on Polyester Fiber-Reinforced Polymer Concrete

Gonzalo Martínez-Barrera [1,*], Miguel Martínez-López [2] and Juan Enrique Martínez-Martínez [3]

[1] Laboratorio de Investigación y Desarrollo de Materiales Avanzados (LIDMA), Facultad de Química, Universidad Autónoma del Estado de México, Toluca 50200, Estado de México, Mexico
[2] División de Ingeniería Industrial e Ingeniería en Energía y Desarrollo Sostenible, Universidad Politécnica del Valle de Toluca, Almoloya de Juárez 50904, Estado de México, Mexico; oroshi_mml@hotmail.com
[3] Escuela Superior de Ingeniería y Tecnología, Universidad Internacional de La Rioja (UNIR), 26006 La Rioja, Spain; juanenrique.martinez@unir.net
* Correspondence: gonzomartinez02@yahoo.com.mx; Tel.: +52-5551843931

Abstract

In the construction industry, there is a growing demand for materials with mechanical properties that surpass those of conventional options. Polymer concrete, composed of polymer resins and mineral aggregates, exhibits superior mechanical performance compared to traditional cement-based concrete. However, its relatively low ductility limits its application in load-bearing structures. To address this limitation, reinforcements such as polyester fibers can be incorporated to enhance ductility. Additionally, gamma radiation has been shown to effectively improve the toughness of polymer concrete. In this study, the effects of marble particle size (0.71, 1.4, and 2.36 mm), polyester fiber content (0.1, 0.3, and 0.5 wt%), and gamma radiation dose (50, 100, and 150 kGy) on the mechanical properties of polymer concrete were investigated. The results indicate increases in compressive strength, deformation capacity, modulus of elasticity, and dynamic modulus. These improvements are attributed to radiation-induced modifications in the morphology of the polyester resin, polyester fibers, and the overall polymer concrete matrix.

Keywords: polymer concrete; polyester fiber; marble; gamma radiation; mechanical properties

1. Introduction

Polymer matrix composites have achieved widespread success in various technological applications due to their superior properties compared to conventional materials [1,2]. In the construction industry, polymer-based materials are increasingly used to partially or completely replace cementitious matrices. One prominent example is polymer concrete, in which cement is entirely replaced by a polymer resin [3–5]. The most commonly used resins in polymer concrete are unsaturated polyester and epoxy resins, while acrylic and polyurethane resins are employed to a lesser extent. Unsaturated polyester resins typically require a chemical initiator, such as methyl ethyl ketone peroxide, along with accelerators like cobalt salts, to promote polymerization. The aggregates used in polymer concrete consist of fine and coarse mineral materials, including silica sand, river sand, calcium carbonate, bentonite, fly ash, and crushed gravel, among others. The mechanical properties of polymer concrete are influenced by several factors, including the type of resin and curing method, the size and shape of the aggregates, and post-curing treatments [6,7].

In addition, natural or synthetic fibers can be incorporated during the curing process to enhance mechanical properties such as flexural strength, compressive strength, and

Check for updates

Academic Editor: Angelo Luongo

Received: 1 August 2026
Revised: 25 August 2026
Accepted: 1 September 2026
Published: 4 September 2026

Copyright: © 2026 by the authors. Licensee MDPI, Basel, Switzerland. This article is an open access article distributed under the terms and conditions of the Creative Commons Attribution (CC BY) license.

stiffness. Commonly used fibers include steel, aramid, glass, carbon, and nylon [3,8–12]. However, relatively few studies have addressed fiber-reinforced polymer concrete. For instance, basalt and glass fibers have been incorporated at concentrations ranging from 0.5 to 20 wt% in epoxy or polyurethane matrices. The addition of basalt fibers has been reported to increase tensile strength by up to 35%, compressive strength by 10%, and flexural strength by 4.8%. Similarly, the incorporation of silane-treated glass fibers has been shown to significantly enhance mechanical performance, with improvements of up to 225% in flexural modulus, 112% in flexural strength, 39.5% in modulus of elasticity, and 15% in compressive strength. Moreover, glass fibers help reduce crack propagation, thereby increasing the overall stiffness of the composite material [13,14].

Polymers can be modified through physical or chemical methods, including radiation-based techniques involving either non-ionizing radiation (such as ultraviolet, UV) or ionizing radiation (such as gamma rays) [15–18]. When exposed to gamma radiation, polymers absorb photon energy and generate reactive species (free radicals), which initiate chemical reactions that alter the polymer structure. Radiation-based modification offers several advantages over conventional treatment methods, such as chemical and thermal processes, due to its ability to induce chemical reactions without the need for additional reagents or catalysts. Furthermore, it offers shorter curing times, operation at atmospheric pressure and ambient temperature, relatively low cost, and is considered an environmentally friendly process [19–23].

Several studies have investigated the combined effects of gamma radiation and fiber reinforcement on polyester matrix composites. For instance, composites based on polyester resin reinforced with curaua and aramid fibers and exposed to radiation doses of 150–300 kGy exhibited reductions of 61% in flexural strength and 67% in modulus of elasticity [24].

In contrast, polyester composites reinforced with jute fibers and irradiated at lower doses (1–5 kGy) showed significant improvements, with tensile strength increasing by 98% and Young's modulus by 500%, although elongation at break decreased by 67% [25]. Similarly, polyester–sisal fiber composites exposed to low radiation doses (around 5 kGy) demonstrated notable enhancements, including increases of 73% in tensile strength and 91% in flexural strength [26]. Other systems, such as polyester resin composites filled with gypsum and irradiated at doses between 20 and 350 kGy, exhibited a 100% increase in compressive strength, while hardness remained unchanged [27]. These variations in mechanical performance are primarily attributed to radiation-induced modifications in the polymer structure, including chain scission, which reduces molecular weight, and cross-linking reactions within the polymer matrix.

Additional studies have examined the effects of gamma radiation on various polymer-based composites [28–31]. For example, epoxy resin composites [32,33]. Those exposed to gamma doses in the range of 10–50 kGy exhibit improved mechanical properties with increasing radiation dose, including an 11% increase in tensile strength [32]. Similarly, sulfur-based polymer concrete irradiated at higher doses (500–1500 kGy) shows enhancements of up to 35% in compressive strength [34]. In composites produced from recycled polymers reinforced with rice husk fibers and exposed to doses between 25 and 150 kGy, tensile strength increases by 15% and the modulus of elasticity by up to 200% [35]. In contrast, chitosan/natural rubber latex (CS/NRL) composites subjected to gamma radiation doses of 10–100 kGy exhibit a decline in mechanical performance, with reductions of 57% in tensile strength, 32% in elongation at break, and 8% in toughness [36]. These variations in mechanical behavior are associated with radiation-induced changes in the composite structure, where the balance between cross-linking and oxidative degradation governs the overall response of the material.

The observed changes in mechanical properties are attributed to modifications in the polymer matrix structure induced by irradiation. When a polymer is exposed to gamma radiation, four primary processes may occur: cross-linking, degradation, grafting, and curing. Cross-linking involves the transformation of linear polymer chains into a three-dimensional network, whereas chain scission (degradation) leads to a reduction in average molecular weight [17,19–21,37,38].

While previous studies have examined the improvement of the mechanical properties of polymer composites through gamma irradiation or fiber reinforcement independently, the synergistic interaction between aggregate particle size distribution, synthetic fiber content, and high-dose gamma irradiation in unsaturated polyester polymer concrete remains an under-researched area. To address this gap, in this study, polymer concrete specimens were fabricated using polyester resin, marble particles with sizes of 0.71, 1.4, and 2.36 mm, and polyester fibers at contents of 0.1, 0.3, and 0.5 wt%. The specimens were subsequently exposed to gamma radiation at doses of 50, 100, and 150 kGy. The effects of marble particle size, fiber content, and ionizing radiation on the mechanical properties were systematically evaluated and correlated with the corresponding morphological changes.

2. Materials and Methods

2.1. Materials

Unsaturated polyester resin was supplied by the Grupo Químico Industrial, located in Toluca, Mexico. The commercial grade used was MR-300/75C. The properties reported by the manufacturer are summarized in Table 1.

Table 1. Properties of polyester resin.

Properties	Value
Brookfield Viscosity, cPs	100–200
Gel time, min	6–8
Exothermic temperature, °C	145–163
Tensile strength, MPa	86
Modulus of elasticity, GPa	3.2
Flexural strength, MPa	103

Three marble particle sizes were used: 0.71 mm (mesh 25), denoted as (S, small); 1.4 mm (mesh 14), denoted as (M, medium); and 2.36 mm (mesh 8), denoted as (L, large). These sizes were selected to maintain a 1:2:3 size ratio and to promote a uniform distribution of the particles within the resin matrix. Figure 1a presents the marble particle size distribution. The marble aggregates were supplied by Minerales GOSA S.A., located in Atizapán de Zaragoza, Mexico. According to the manufacturer, the material is composed of approximately 90% calcite ($CaCO_3$) and 10% dolomite $CaMg(CO_3)_2$. The corresponding physical and chemical properties are summarized in Table 2.

Table 2. Properties of marble aggregates.

Property	Value
Density, g/cm^3	2.38–2.87
Mohs hardness	3–4
Compressive strength, MPa	58–98
Tensile strength, MPa	10–35

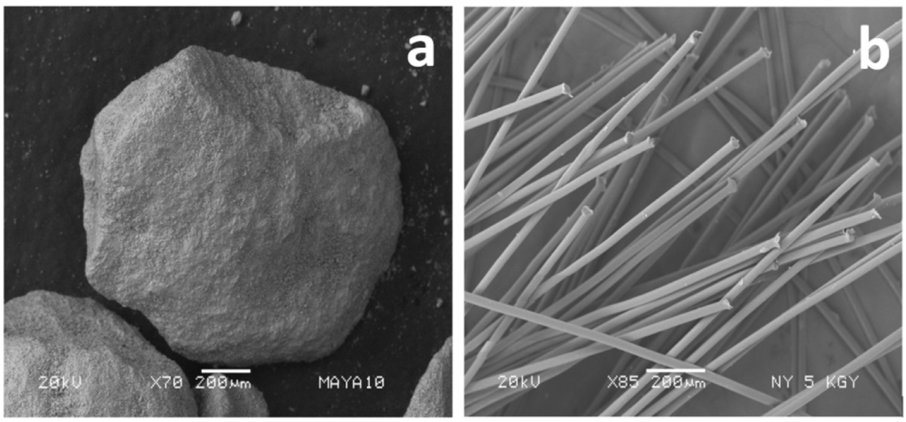


Figure 1. Marble particles (**a**), and polyester fibers (**b**).

The polyester fibers, with a diameter of 30–40 µm and a length of 20 mm (Figure 1b), were supplied by Gütermann Polygal, located in Cuernavaca, Mexico. Their properties are shown in Table 3.

Table 3. Properties of polyester fibers.

Property	Value
Denier	300
Specific gravity	1.36
Moisture absorption, %	0.4
Tensile strength, MPa	44–73
Tensile elongation, %	20
Elongation, %	16

2.2. Polymer Concrete Production

Before the mixing process, the marble particles were oven-dried at 80 °C for 24 h to eliminate residual moisture, as the presence of water during curing can reduce the interfacial adhesion between the composite constituents. In the initial experimental stage, polymer concrete specimens (50 × 50 × 50 mm) were fabricated using 30 wt% unsaturated polyester resin and 70 wt% marble aggregates. Polymerization was initiated with methyl ethyl ketone peroxide (MEKP) at a ratio of 1 mL per 100 g of resin, and curing was carried out at room temperature. The mixing procedure consisted of an initial stage of 1.0 min at 140 rpm, followed by 1.5 min at 285 rpm. The specimens were then cured at 23.0 ± 3.0 °C for 24 h.

In each polymer concrete formulation, two marble particle sizes were combined: (i) 0.71 and 1.4 mm, denoted as the S–M (small–medium) combination; (ii) 0.71 and 2.36 mm, denoted as the S–L (small–large) combination; and (iii) 1.4 and 2.36 mm, denoted as the M–L (medium–large) combination. For each size combination, a 1:1 weight ratio was maintained. For each radiation dose (control, 50, 100, and 150 kGy), five specimens were prepared for each formulation presented in Table 4. A total of 240 specimens were produced for this study.

In the second experimental stage, polyester fibers were incorporated at 0.1, 0.3, and 0.5 wt% into the polyester resin–marble particle mixtures, partially replacing the marble content. For each fiber content five specimens were prepared. The corresponding mix compositions are presented in Table 4.

Table 4. Polymer concrete formulations.

Polymer Concrete	Resin (%)	S-M Marble (%)	S-L Marble (%)	M-L Marble (%)	Polyester Fiber (%)
R-SM	30	70	-	-	-
R-SM-0.1F	30	69.9	-	-	0.1
R-SM-0.3F	30	69.7	-	-	0.3
R-SM-0.5F	30	69.5	-	-	0.5
R-SL	30	-	70	-	-
R-SL-0.1F	30		69.9	-	0.1
R-SL-0.3F	30	-	69.7	-	0.3
R-SL-0.5F	30	-	69.5	-	0.5
R-ML	30	-	-	70	-
R-ML-0.1F	30	-	-	69.9	0.1
R-ML-0.3F	30	-	-	69.7	0.3
R-ML-0.5F	30	-	-	69.5	0.5

2.3. Gamma Irradiation of Polymer Concrete, Polyester Resin and Polyester Fibers

In separate experiments, polyester resin, polyester fibers, and polymer concrete samples were irradiated. Each material was exposed to gamma radiation at doses of 50, 100, and 150 kGy in air at room temperature, using a cobalt-60 source with a dose rate of 3.5 kGy/h. Irradiation was carried out in a JS-6500 industrial irradiator located at the National Institute of Nuclear Research of Mexico (ININ). A dyed polymethyl methacrylate (PMMA) dosimeter was used to monitor the absorbed dose.

2.4. Mechanical Testing

Compression tests were performed on polymer concrete specimens using a Controls™ model 70-S17C2 universal testing machine (Cernusco, Italy), equipped with a 30-ton load cell. Compression tests were conducted in accordance with ASTM C579-23. The static modulus of elasticity (E) was determined using data from the compression tests. Recorded load-versus-displacement measurements were used to calculate stress (σ) and strain (ε). Subsequently, the elastic modulus was evaluated as the slope of the linear elastic region of the stress–strain response. The dynamic modulus of elasticity was recorded using a Controls™ model 58-E0048 ultrasonic pulse velocity tester (Cernusco, Italy), with an ultrasonic resolution of 0.1 ms. The dynamic modulus is calculated from the equation $Ed = v2m\ (1 + p)(1 - 2p)/(1 - p)$, where v is the pulse velocity, m is the mass density, and p is Poisson's ratio.

2.5. Morphological Characterization

Polyester resin, polyester fibers, and small fragments from the fracture zone obtained after compression testing were vacuum-coated with carbon layers of 3 and 10 nm thickness using an E.F. Fullam vacuum evaporator at 50 mTorr. The surfaces of both non-irradiated and irradiated samples were then examined by scanning electron microscopy (SEM) using a JEOL JSM-6510LV microscope. The instrument, equipped with a factory-precentered filament and a high-voltage resolution of 3.0 nm, was operated at an accelerating voltage of 20 keV. All images were acquired in secondary electron mode.

3. Results and Discussion

The results for four mechanical properties—compressive strength, ultimate compressive strength, compressive modulus, and dynamic modulus—were evaluated. Each property was analyzed based on: (i) the combination of marble particle size and fiber content;

(ii) the combination of marble particle size and radiation dose; and (iii) the combined effects of marble particle size, fiber content and radiation dose.

3.1. Compressive Strength

3.1.1. Marble Particle Size and Fiber Content

For plain polymer concrete (i.e., without polyester fibers), the compressive strength ranges from 58.0 to 62.3 MPa, as shown in Figure 2 (error bars indicate the standard deviation). For fiber-reinforced polymer concrete: (i) In terms of particle size combinations, the small–large (S–L) mixture exhibited the highest strength, followed by the small–medium (S–M) combination. (ii) With respect to polyester fiber content, compressive strength values range from 54.3 to 61.9 MPa. An initial decrease is observed at 0.3% fiber content, followed by a slight increase at 0.5% for the small-large (S–L) and medium–large (M–L) combinations. In contrast, for the (S–M) combination, strength gradually decreases with increasing fiber content. Overall, the incorporation of fibers tends to reduce compressive strength, regardless of the marble particle size.

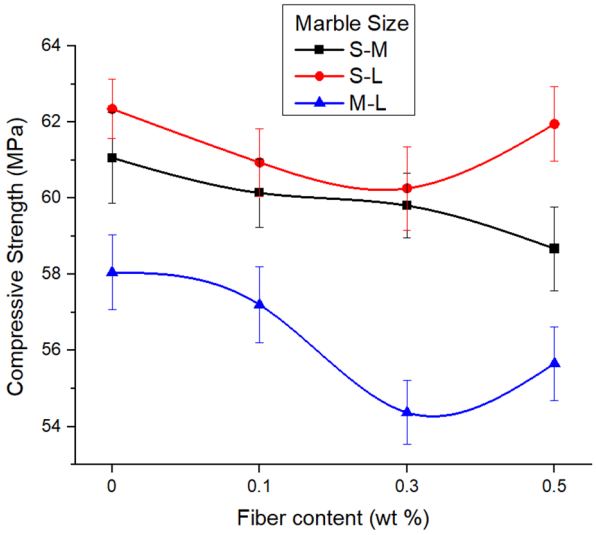


Figure 2. Compressive strength of polymer concrete with and without polyester fiber reinforcement.

The slight to moderate reduction in compressive strength observed following the incorporation of polyester fibers (particularly at proportions of 0.3% and 0.5% by weight) can be attributed to three main physical and microstructural mechanisms:

(i) Fiber entanglement and induced microporosity. At higher fiber contents (0.3 and 0.5 wt%), flexible synthetic fibers tend to form localized agglomerations or entanglements during mechanical mixing. These fiber agglomerates trap air microbubbles during casting, resulting in localized micro-voids within the cured polyester matrix. Under compressive loads, these micro-voids act as stress concentration points, reducing the effective load-bearing cross-sectional area.

(ii) Soft-inclusion mechanical behavior under compressive loading. Unlike tensile or flexural stress states (where fibers effectively bridge crack surfaces and carry tensile loads), under compressive loading, the specimen undergoes lateral expansion due to Poisson's ratio effects [39]. Flexible polymeric fibers possess lower transverse stiffness compared to the rigid cured polyester resin matrix and marble aggregates. Consequently, the embedded fibers act as compliant "soft inclusions" or mechanical discontinuities, offering minimal lateral confinement and facilitating localized shear band formation.

(iii) Shear discontinuity at the interface. Polyester fibers rely primarily on physical-mechanical interlocking with the polyester resin matrix. Under compressive loads, shear stresses develop along the fiber-matrix interface. A weak interfacial bond promotes localized shear separation along the fiber, initiating microcracking prior to matrix crushing [40–45]. Overall, the highest compressive strength for fiber-reinforced concretes was achieved with the highest fiber content (5%) and the S–L particle size combination, reaching 61.9 MPa. It is worth noting that this value was statistically significant only when compared to the concrete containing the M–L particle size combination.

Another option for analyzing the data in Figure 2 is the Response Surface Methodology (RSM), a statistical technique used to address and optimize problems in which a response variable is influenced by multiple independent variables. In this work, the input variables are listed in Table 5.

Table 5. Input variables for the Response Surface Methodology (RSM).

Input Variable	Units	Values
Particle size	mm	0.71; 1.4; 2.36
Polyester fibers	%	0; 0.1; 0.3; 0.5
Radiation dose	kGy	0; 50; 100; 150

Figure 3 shows the 3D response surfaces that correlate two independent variables (marble particle size and fiber content), with their resulting response (compressive strength). In this figure, concrete with small-large particles (S-L), have the maximum values, while those with small-medium (S-M) or medium-large (M-L) particles have low compressive strength values.

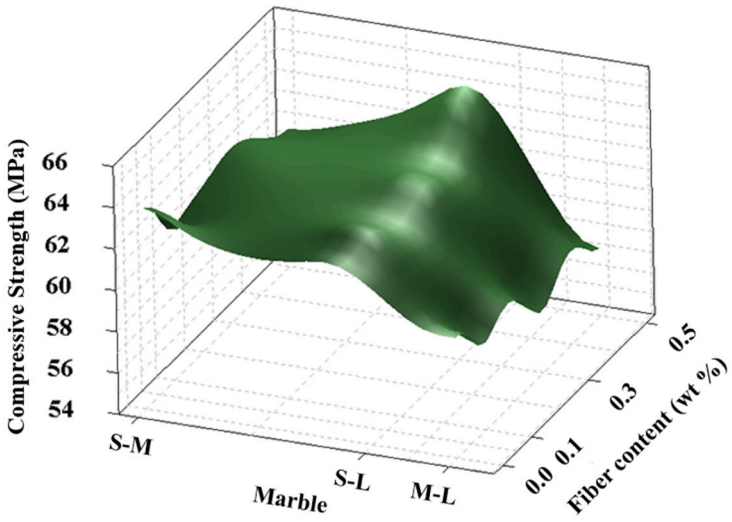


Figure 3. Response Surface of compressive strength as a function of particle size and polyester fiber content.

3.1.2. Marble Particle Size and Radiation Dose

Figure 4 shows the compressive strength values of the non-irradiated and irradiated polymer concrete. For the irradiated polymer concrete: (i) In terms of particle size combinations, concrete with small–medium (S–M) exhibited the highest strength, followed concrete with small–large (S–L) combination. Concrete with small-medium particles has more contact points between the particles and the polyester resin. (ii) With respect to radiation dose, the compressive strength values ranged from 58.1 to 65.5 MPa. The values increased

gradually with increasing radiation dose, regardless of the marble particle size combinations. The maximum compressive strength of 65.5 MPa was obtained after irradiation at a dose of 150 kGy using the S–M particle size combination. This value represented a 6.5% improvement compared to non-irradiated concrete with the same particle size combination (S–M). The cross-linked chains in the resin generate greater stress transfer with the marble particles after irradiation, thus increasing compressive strength. Hidayat et al. discovered that a recycled polymer exposed to gamma radiation and subsequently added to concrete, after irradiation, caused crosslinking of the polymer chains and an increase in crosslinking density. These characteristics resulted in increased compressive strength [46].

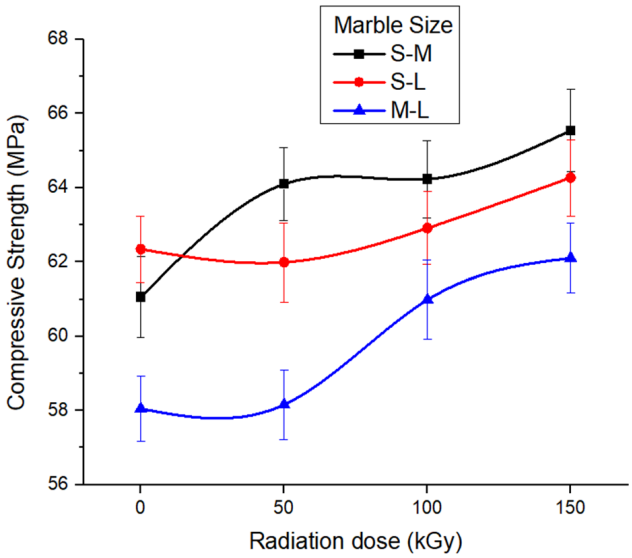


Figure 4. Compressive strength of non-irradiated and irradiated polymer concrete.

Figure 5 shows the 3D response surfaces that correlate the size of the marble particles with the applied radiation doses and their responses (compressive strength). As can be observed, increased radiation leads to higher compressive strength. It is also worth noting that the highest values were obtained with concretes containing small- and medium-sized particles (S-M).

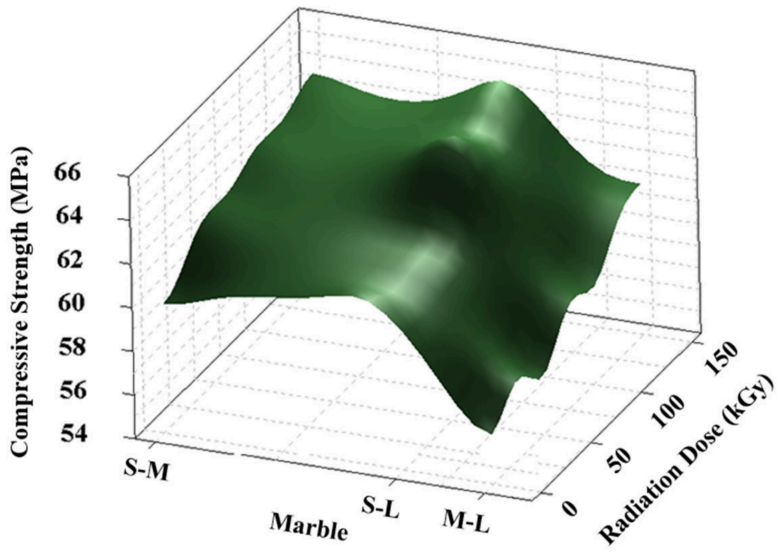


Figure 5. Response surface for compressive strength as a function of the particle size and radiation dose.

The observed mechanical improvements can be attributed to structural modifications induced by gamma radiation in the polyester resin, as illustrated in Figure 6. The unirradiated resin (Figure 6a) exhibits a relatively smooth surface with minimal roughness (as indicated by the arrows), unlike the irradiated samples (Figure 6b,c), which show progressively greater surface irregularities. As the radiation increases, noticeable surface deterioration occurs, characterized by the formation of cracks (highlighted with circles) and cavities (marked with ovals). These features promote greater interfacial interaction and enhanced mechanical interlocking between the resin matrix, marble particles, and reinforcing fibers, ultimately contributing to improved compressive strength.

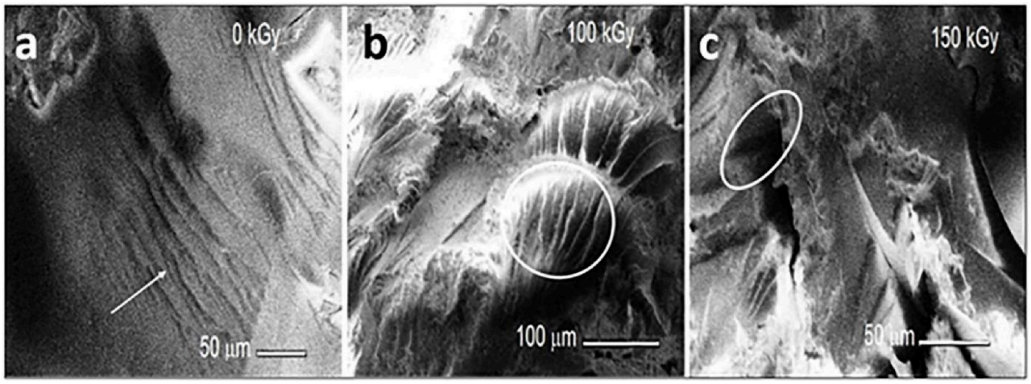


Figure 6. SEM micrographs of polyester resin (**a**) non-irradiated, and (**b**,**c**) irradiated.

3.1.3. Marble Particle Size, Fiber Content and Radiation Dose

Representing the compressive strength of the concrete in a single figure is challenging due to the combined influence of multiple variables, namely marble particle size, polyester fiber content, and gamma radiation dose. Nevertheless, these results are summarized in Figure 7.

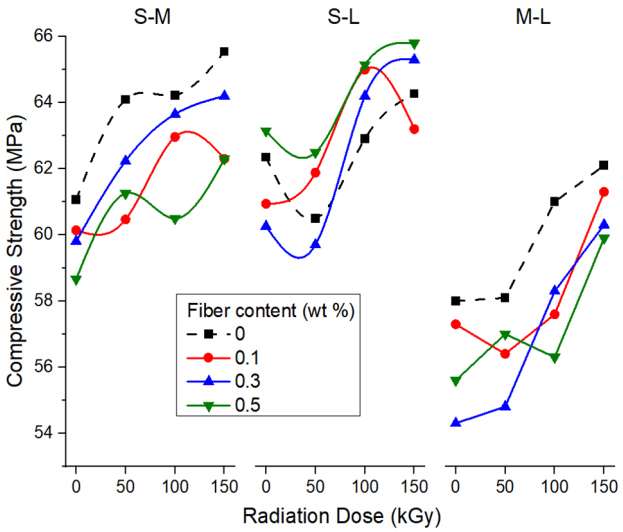


Figure 7. Compressive strength of non-irradiated and irradiated polymer concrete as a function of marble particle size, polyester fiber content, and gamma radiation dose.

(i) With respect to marble particle size, the highest compressive strength values were obtained for concretes incorporating a small-large (S–L) particle size distribution, followed by those with small-medium (S–M) and medium-large (M–L) combinations, respectively.

(ii) In terms of fiber content, the results exhibit significant variability and do not follow a monotonic trend. The highest values are observed at 0.5% fiber content, after which the compressive strength decreases with increasing fiber content.

(iii) With respect to radiation dose, a consistent increase in compressive strength is observed as the dose increases. The measured values range from 54.3 to 65.8 MPa, with the highest strength achieved at a dose of 150 kGy. This corresponds to an improvement of approximately 21.1% compared to the non-irradiated concrete.

Although the incorporation of fillers into composite materials is generally associated with a reduction in compressive strength, the application of gamma radiation counteracts this effect by improving mechanical performance. Furthermore, a greater separation between the marble particles and the resin matrix appears to promote radiation-induced crosslinking, thereby contributing to increased strength.

The 3D response surfaces illustrating the relationship between gamma radiation dose, polyester fiber content, and compressive strength are presented in Figure 8. Two main trends can be identified: (i) compressive strength increases with increasing radiation dose, which can be attributed to radiation-induced crosslinking of polymer chains; and (ii) compressive strength decreases as fiber content increases, likely due to inadequate fiber dispersion within the matrix.

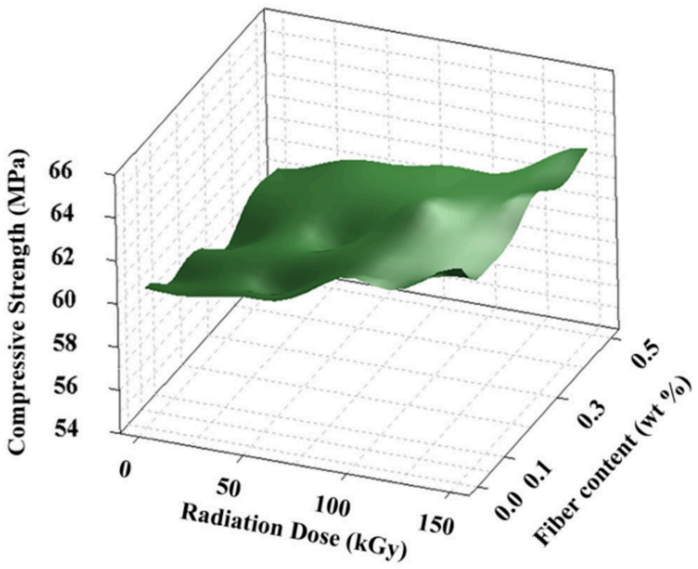


Figure 8. Response Surface of compressive strength as a function of gamma radiation dose and polyester fiber content.

3.2. Ultimate Compressive Strain

3.2.1. Marble Particle Size and Fiber Content

For plain polymer concrete (i.e., without polyester fibers), the ultimate compressive strain ranges from 0.0644 to 0.0652 mm/mm, as shown in Figure 9. In fiber-reinforced polymer concrete, two main trends are observed. (i) First, regarding particle size combinations, the highest deformations are obtained with small–medium (S–M) particles. (ii) Second, in terms of polyester fiber content, deformation values range from 0.0648 to 0.0692 mm/mm. Overall, the incorporation of fibers increases deformation up to a content of 0.3 wt%; however, at a higher content (0.5 wt%), a slight decrease is observed. In summary, the maximum deformation, namely 0.0695 mm/mm, occurs in concrete with S–M particles and 0.3 wt% fibers, representing a 7.9% increase compared to plain polymer concrete.

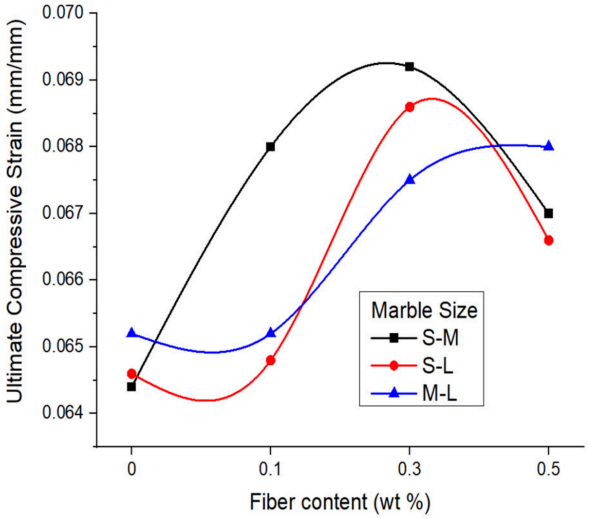


Figure 9. Ultimate compressive strain of polymer concrete reinforced with polyester fibers.

According to the response surface methodology (RSM), the highest deformation values are observed in concrete containing small–medium (S–M) sized particles and 0.3 wt% polyester fibers (Figure 10). These results indicate that fiber content is a key parameter influencing deformation, such that a higher polyester fiber content leads to greater deformation capacity.

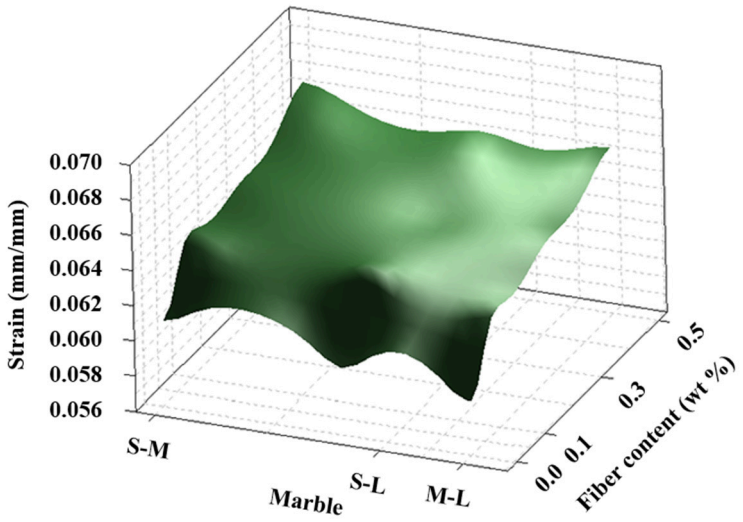


Figure 10. Response surface of compressive strain as a function of particle size and polyester fiber content.

3.2.2. Marble Particle Size and Radiation Dose

Figure 11 presents the ultimate compressive strain values for both non-irradiated and irradiated polymer concrete. For the irradiated samples: (i) the deformation values range from 0.0564 to 0.0616 mm/mm, with the concrete containing the small–medium (S–M) particle combination exhibiting the highest strain; and (ii) exposure to gamma radiation leads to a reduction in deformation, as all irradiated samples show lower strain values than their non-irradiated counterparts. The minimum value reached 0.0564 mm/mm, corresponding to a decrease of approximately 13% relative to the non-irradiated concrete. This behavior suggests that gamma radiation induces cross-linking of the polymer chains, resulting in reduced deformability of the material. Kiss et al. found that in rubber compounds, tensile

strength, elongation at break, modulus, and Shore A hardness decrease with increasing radiation dose [47].

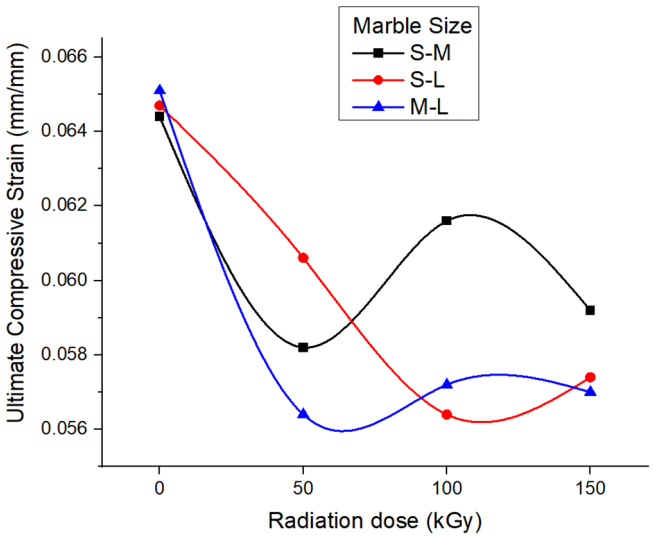


Figure 11. Ultimate compressive strain of non-irradiated and irradiated polymer concrete.

The response surface indicates that the highest deformation values occur in unirradiated concretes, whereas the lowest are observed in samples irradiated at 50 and 100 kGy (Figure 12). These results suggest that gamma irradiation reduces deformation, thereby improving the ductility of the polymer concrete.

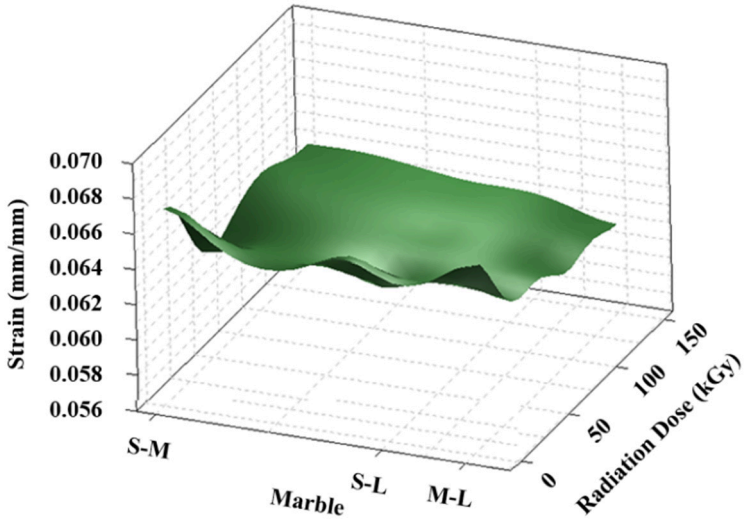


Figure 12. Response Surface of compressive strain as a function of particle size and radiation dose.

3.2.3. Marble Particle Size, Fiber Content and Radiation Dose

The ultimate compressive strain values for polymer concretes incorporating combined marble particle sizes, polyester fibers, and gamma irradiation are presented in Figure 13. (i) Regarding particle size, the lowest deformation values were obtained for concretes with a medium–large (M–L) particle combination. (ii) In terms of fiber content, minimum deformation occurred at 0.3% fiber addition. (iii) Regarding the radiation dose, a gradual decrease in deformation was observed as the dose increased, regardless of particle size distribution or fiber content. Overall, the measured values ranged from 0.0564 to 0.0692 mm/mm.

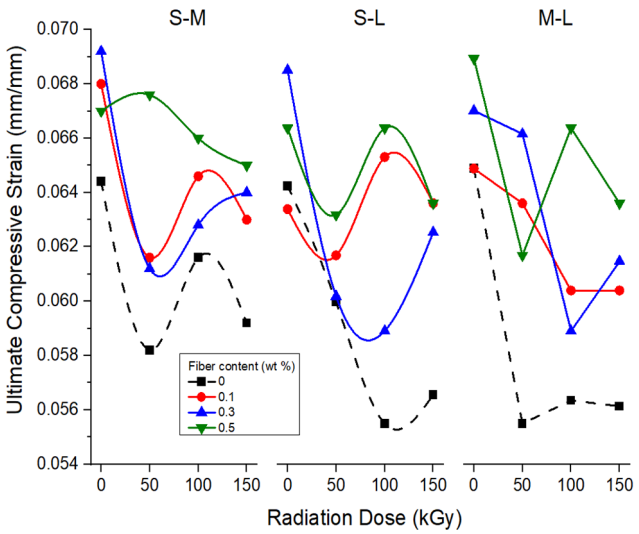


Figure 13. Ultimate compressive strain of non-irradiated and irradiated polymer concrete as a function of marble particle size, polyester fiber content, and gamma radiation dose.

The highest deformation was recorded for concrete containing a small–medium (S–M) particle combination, 0.5% fibers, and irradiated at 50 kGy. In contrast, a reduction of up to 13% was observed for concrete with a medium–large (M–L) particle combination, 0.3% fibers, and irradiated at 100 kGy. These results indicate that higher radiation doses, lower fiber content, and larger marble particle sizes contribute to a significant reduction in deformation. Alhazmi et al. [48] reported that the incorporation of waste and recycled materials into polymer concrete may result in poor adhesion between the polymer matrix and tire particles, consequently leading to lower mechanical performance.

The variations in compression deformation observed in Figure 13 are more clearly visualized in the 3D response surface shown in Figure 14, which relates radiation dose to fiber content. This representation highlights distinct regions of maximum (peaks) and minimum (valleys) values, allowing for a clearer identification of the interaction effects between these variables.

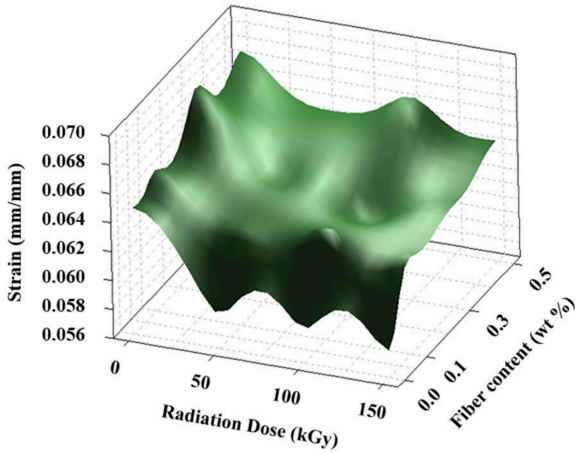


Figure 14. Response surface of compressive strain as a function of fiber content and radiation dose.

Variations in compressive deformation depend largely on fiber content; therefore, in a separate experiment, polyester fibers were irradiated, and the resulting surface modifications (Figure 15) were correlated with the observed mechanical behavior. Figure 15 shows that as the radiation dose increases, a greater number of particles appear on the fiber surface (indicated by the arrows). These features can act as anchoring points between the

fiber and the resin, thereby reducing deformation during the compression test. Furthermore, radiation induces an increase in surface roughness (indicated by the oval), which increases the number of contact points at the fiber–matrix interface and further contributes to reducing deformation.

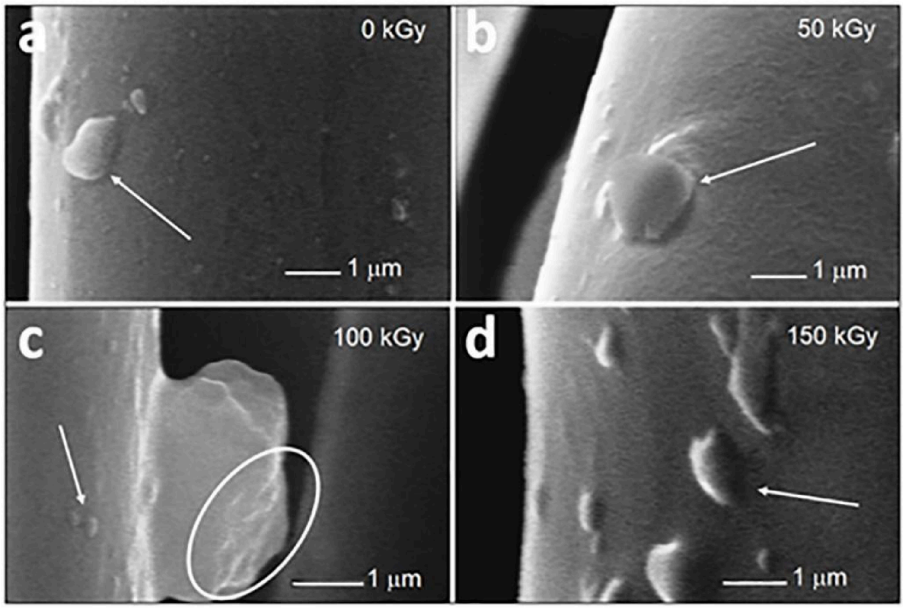


Figure 15. SEM images of polyester fibers: (**a**) unirradiated, and (**b**–**d**) gamma-irradiated.

3.3. Compressive and Dynamic Modulus

3.3.1. Marble Particle Size and Fiber Content

Figure 16 presents the two types of modulus of elasticity measured for polymer concretes: (i) compressive modulus and (ii) dynamic modulus. In the case of compressive modulus, for plain concrete, the compressive modulus ranges from 8.8 to 9.7 GPa. In fiber-reinforced concrete, the highest modulus value, namely 9.4 GPa, was obtained for concrete with small–medium (S–M) particle size combination, and 0.3% fibers. Conversely, increasing the polyester fiber content leads to a gradual decrease in the modulus, regardless of the marble particle size distribution. Overall, smaller particle sizes combined with lower fiber contents favor higher elastic modulus values [49,50].

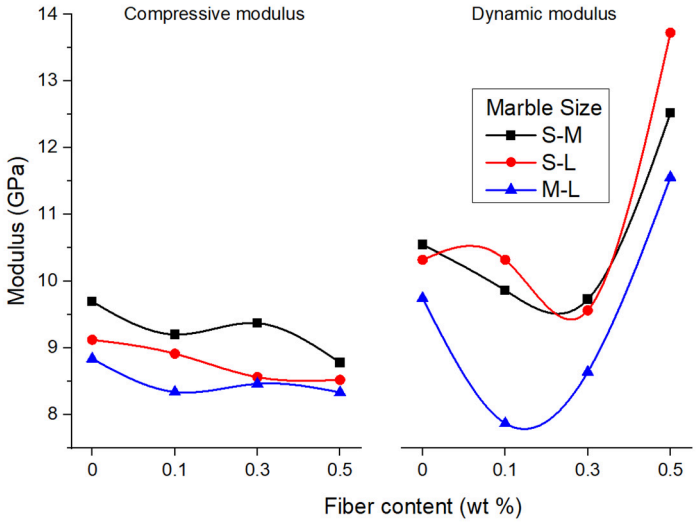


Figure 16. Compressive Modulus and Dynamic Modulus of Polyester Fiber-Reinforced Polymer Concrete.

A different trend is observed for the dynamic modulus. For plain concrete, the values range from 9.75 to 10.54 GPa, which are higher than those obtained for the compressive modulus. In fiber-reinforced concrete, the values range from 7.86 to 13.72 GPa. The concrete with small–large (S–L) particle combination and 0.5% fiber exhibits the highest modulus values. In contrast, the modulus decreases at fiber contents of 0.1% and 0.3%, but increases markedly at higher fiber contents, regardless of the marble particle size distribution. The highest values were obtained with a fiber content of 0.5% combined with the small–large (S–L) particle configuration, resulting in a maximum improvement of 32% compared to plain concrete.

As is well established, the dynamic modulus is determined through non-destructive ultrasonic test, in which wave propagation is influenced by the material's constituent phases: in this case, marble aggregates, polyester resin, and polyester fibers. In conventional concrete, dynamic modulus values are typically higher than those obtained from compression tests, yet both tend to exhibit similar trends.

In this study, however, the compressive and dynamic moduli show comparable behavior at fiber contents of 0.1 and 0.3 wt%, where both decrease. This trend does not persist at 0.5 wt% fiber content, where the dynamic modulus increases markedly. This behavior suggests that a higher fiber content intensifies interactions with ultrasonic waves, promoting greater wave transmission and vibration within the concrete which translates into apparent increase in the measured modulus of elasticity.

Figure 17 shows the three-dimensional response surfaces of the modulus of elasticity as a function of particle size and fiber content. As can be seen, for the compressive modulus, the highest values correspond to concrete with small and medium (S-M) particles and lower polyester fiber content. In contrast, in the case of the dynamic modulus, the contribution of the polyester fibers is significant, as higher fiber content results in the highest values.

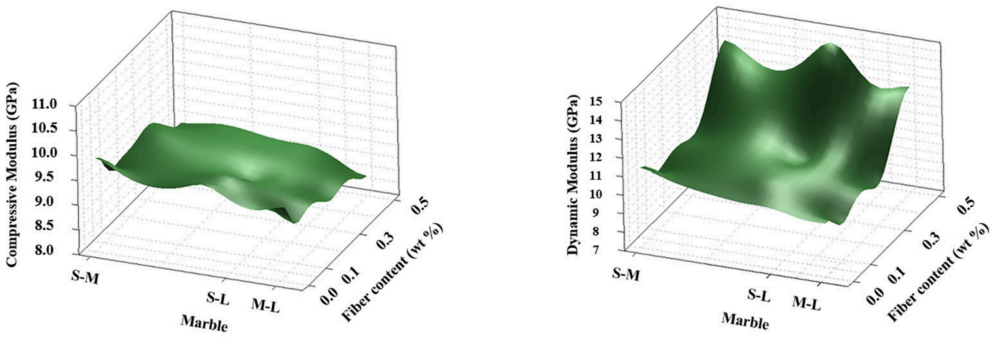


Figure 17. Response surface analysis of the compressive and dynamic moduli as functions of particle size and polyester fiber content.

3.3.2. Marble Particle Size and Radiation Dose

Figure 18 presents the modulus of elasticity for both non-irradiated and irradiated polymer concrete. For irradiated specimens, the compressive modulus exhibited the following trends: (i) regarding particle size distribution, mixtures with small–medium (S–M) particles showed the highest modulus values; and (ii) in terms of radiation dose, values ranged from 9.6 to 10.55 GPa. The modulus increased with dose up to 50 kGy and decreased at higher doses, regardless of the marble particle size combination. The maximum value, 10.55 GPa, was obtained for concrete with S-M particles and irradiated at 50 kGy, representing an 8.8% increase compared to non-irradiated concrete. This improvement is attributed to gamma radiation–induced chain scission in the resin, which enhances stiffness [51,52]. Exposures to irradiation at higher doses, recombination of polymer chains becomes dominant, leading to a reduction in the modulus of elasticity. Chayoukhi et al.

mention that higher doses produce changes in properties, which are attributed to the increased number of cross-links generated in the network as the absorbed dose increases. Furthermore, cross-linking restricts the mobility of the polymer chains and results in an increase in density [53]. Furthermore, in composite materials containing acrylic resin, at low doses of radiation, compressive strength increases by 104% due to crosslinking of the polymer chains. However, at higher doses, strength is negatively affected due to breakage of the polymer chains [54].

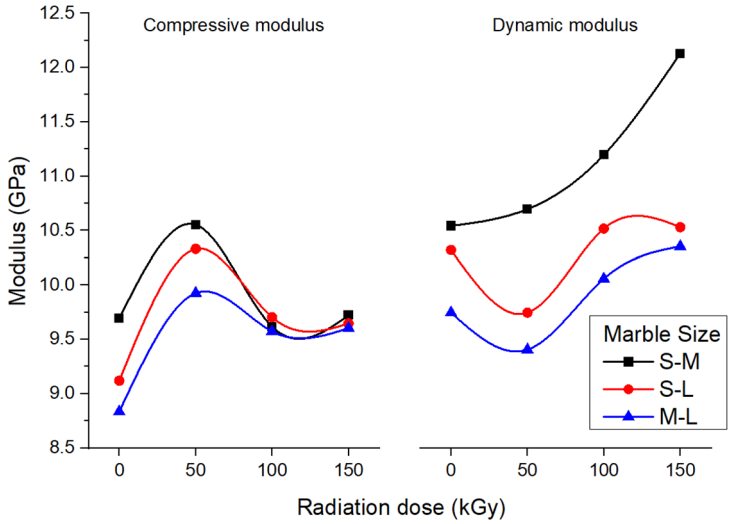


Figure 18. Compressive and dynamic moduli of unirradiated and gamma-irradiated polymer concrete.

The dynamic modulus showed a different trend from the compression modulus, with values increasing or decreasing as the radiation dose increased. At higher radiation doses, increased cross-linking of the polymer chains in the polyester resin improves stress transfer between the matrix and the fibers, resulting in an increase in the dynamic modulus. The maximum value, 12.1 GPa, was observed for concrete with small–medium (S–M) particles and irradiated at 150 kGy, representing a 15% increase compared to the non-irradiated material. Polymer composite materials were irradiated at low doses, and their Young's modulus increased. These improvements are due to the disruption of chemical bonds caused by gamma rays and the formation of new ones; this generates more active sites, resulting in better interfacial bonding [55].

The response surface reveals a well-defined trend. For the compressive modulus, the highest values are obtained at a radiation dose of 50 kGy using small–medium (S–M) particles (Figure 19), indicating a stiffer material characterized by high stress capacity and low deformation. In contrast, the dynamic modulus reaches its maximum for the same particle size combination (S–M) but at a higher dose of 150 kGy. These results suggest that gamma radiation–induced modifications to the polyester resin increase the stiffness of the concrete, with the optimal dose depending on the mechanical property under considered.

The modulus of elasticity of polymer concrete can be correlated with the fracture surface observed after the compression test, as shown in Figure 20. Fractured marble particles are observed within the matrix (highlighted by circles), indicating that the failure propagated through the aggregates. This behavior is attributed to the high compressive stresses applied during testing and occurs more frequently in the irradiated specimens. The effect is associated with radiation-induced cross-linking and chain scission in the polyester resin, with the predominant mechanism depending on the radiation dose. At 50 kGy—the dose at which the highest modulus of elasticity is observed—chain scission appears to prevail, enhancing the interfacial bonding between the resin and marble particles.

This improved interaction reduces deformation and leads to an increase in the modulus of elasticity.

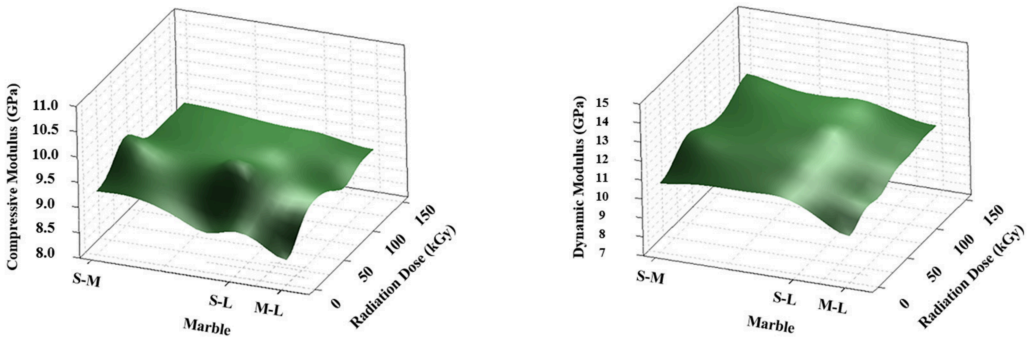


Figure 19. Response surface analysis of compressive and dynamic moduli as functions of particle size distribution and radiation dose.

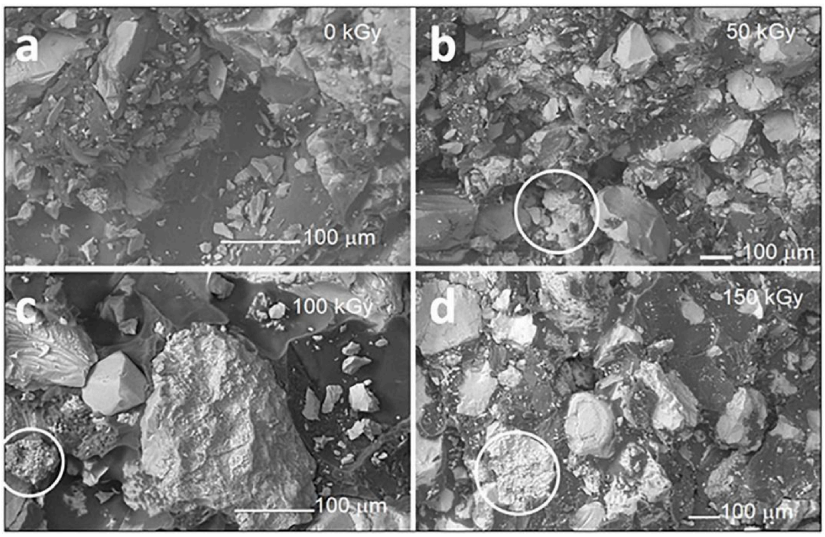


Figure 20. SEM images of polymer concrete: (**a**) unirradiated, and (**b**–**d**) gamma-irradiated.

3.3.3. Marble Particle Size, Fiber Content and Radiation Dose

Figure 21 presents the compressive and dynamic modulus of unirradiated and irradiated polyester fiber-reinforced polymer concrete. In the case of the compressive modulus, all measured values are lower than those of plain concrete. (i) With respect to marble particle size combination, the highest moduli were obtained for concrete with small–medium particles (S–M). (ii) In terms of fiber content, the optimum value corresponds to 0.1 wt% polyester fiber. (iii) Regarding radiation dose, the effect is dose-dependent: the modulus increases at 50 kGy, decreases at 100 kGy, and in some cases increases again at 150 kGy. Overall, the maximum modulus (9.8 GPa) was achieved for concrete with small–large particles (S–L), 0.1 wt% polyester fibers, and irradiation at 150 kGy, representing a 7.6% increase compared to unirradiated concrete. These results indicate that a combination of low fiber content and higher radiation doses contributes to obtaining a more rigid polymer concrete.

For the dynamic modulus, the following trends were observed: (i) the highest values correspond to mixtures with small–large particles (S–L); (ii) regarding fiber content, two distinct behaviors are evident, at 0.1 wt% and 0.3 wt% fiber, the modulus is lower than that of plain concrete, whereas at 0.5 wt% fiber, the values exceed those of the unreinforced material; and (iii) the effect of radiation dose is non-uniform. In some cases, the dynamic modulus increases with increasing dose, while in others it rises to 50 kGy, decreases at 100 kGy, and increases again at 150 kGy. Overall, the maximum modulus (14.8 GPa)

was achieved for concrete with small–large particles (S–L), 0.5 wt% polyester fibers, and irradiation at 100 kGy, representing a 42.3% increase compared to unirradiated concrete. Dynamic modulus values obtained through ultrasonic testing differ from those measured under compression. At higher fiber contents, an increased interaction between the fibers and the ultrasonic waves improves wave propagation characteristics, resulting in higher apparent concrete stiffness.

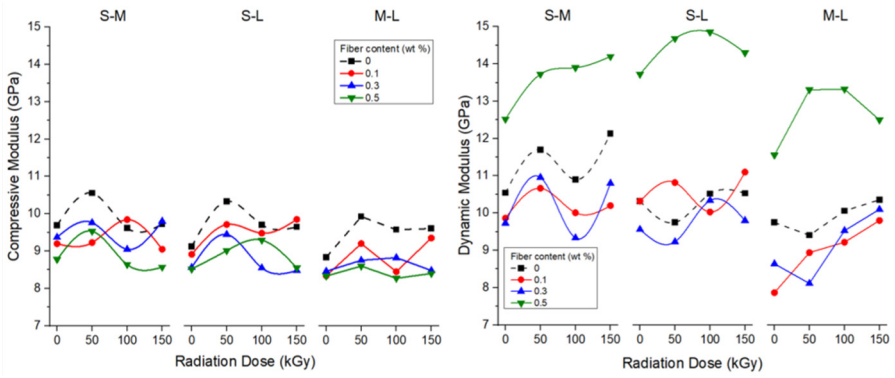


Figure 21. Modulus of elasticity of fiber-reinforced polymer concrete under unirradiated and gamma-irradiated conditions.

Figure 22 presents the response surface relating radiation dose and fiber content to the modulus of elasticity. For the compressive modulus, pronounced peaks are observed at 50 kGy, whereas a noticeable reduction occurs at 100 kGy. In contrast, the dynamic modulus shows a markedly different trend, with higher peaks associated with higher fiber content.

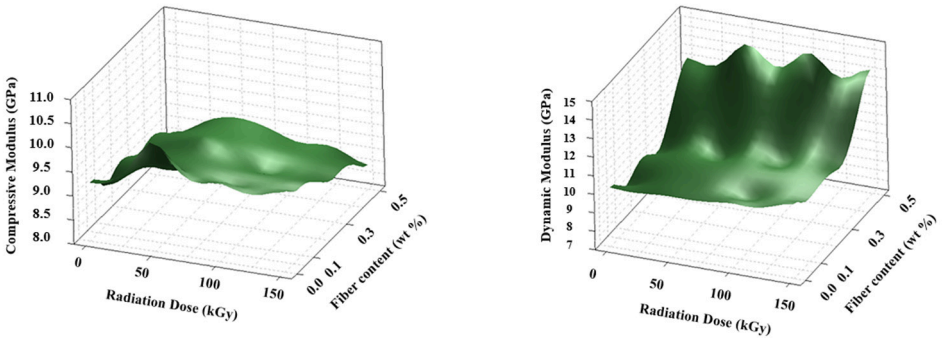


Figure 22. Response surface analysis of compressive and dynamic moduli as functions of fiber content and radiation dose.

In summary, the highest values for strength, strain, compressive and dynamic moduli are presented in Table 6.

Table 6. Comparison of the highest mechanical values of polymer concretes.

Type of Concrete	Strength				Strain				Compressive Modulus				Dynamic Modulus			
	MPa	M	%f	kGy	mm/mm	M	%f	kGy	GPa	M	%f	kGy	GPa	M	%f	kGy
PC	62.3	S–L	-	-	0.0652	S–M	-	-	9.7	S–M	-	-	10.5	S–M	-	-
IPC	65.5	S–M	-	150	0.0616	S–M	-	100	10.5	S–M	-	50	12.1	S–M	-	150
CPF	61.9	S–L	0.5	-	0.0692	S–M	0.3	-	9.4	S–M	0.3	-	13.7	S–L	0.5	-
CPFI	65.8	S–L	0.5	150	0.0692	S–M	0.5	50	9.8	S–L	0.1	150	14.8	S–L	0.5	100

PC = Plain concrete; IPC = Irradiated plain concrete; CPF = Concrete with polyester fibers; CPFI = Concrete with polyester fibers and irradiated.

4. Conclusions

Based on the highest values reported for polymer concrete (Table 6), the effects of marble particle size, polyester fiber content, and gamma radiation dose can be identified. Maximum compressive strength was achieved using a small–large (S–L) particle distribution, 0.5% polyester fiber, and a radiation dose of 150 kGy. In contrast, deformation exhibited a different trend: the highest values were obtained with small–medium (S–M) particles, fiber contents of 0.3–0.5%, and radiation doses of 50–100 kGy. This indicates that the deformation is more sensitive to variations in particle size, fiber content, and moderate radiation levels. Significant differences in the modulus of elasticity were also observed. The compressive modulus reached its highest values with small–medium (S–M) particles, 0.1–0.3% fiber content, and radiation doses of 50 or 150 kGy. Similarly, the dynamic modulus was maximized with both small–medium (S–M) and small–large (S–L) particles, combined with 0.5% fiber content and radiation doses of 100–150 kGy. Overall, the use of small–medium (S–M) particles tends to enhance both compressive strength and compressive modulus, likely due to the increased surface area between components. Lower fiber content promotes greater deformation and a higher compression modulus, contributing to increased deformability. Finally, higher radiation doses (150 kGy) lead to an increase in compressive strength and dynamic modulus, indicating that gamma irradiation enhances the hardness and strength of polymer concrete. This improvement is primarily attributed to the cross-linking of polymer chains, which strengthens interfacial interactions within the composite material.

Author Contributions: Conceptualization, G.M.-B., M.M.-L. and J.E.M.-M.; methodology, G.M.-B. and M.M.-L.; validation, G.M.-B. and M.M.-L.; formal analysis, G.M.-B. and M.M.-L.; investigation, G.M.-B. and M.M.-L.; data curation, G.M.-B., M.M.-L. and J.E.M.-M.; writing—original draft preparation, G.M.-B., M.M.-L. and J.E.M.-M.; writing—review and editing, G.M.-B., M.M.-L. and J.E.M.-M.; project administration, G.M.-B. All authors have read and agreed to the published version of the manuscript.

Funding: This research received no external funding.

Data Availability Statement: All data, models, and code generated or used during the study appear in the article.

Acknowledgments: We would like to thank the National Council for Science, Humanities and Technology of Mexico (CONAHCYT) for supporting the Graduate Program in Materials Science at the Autonomous University of the State of Mexico (UAEM).

Conflicts of Interest: The authors declare no conflicts of interest.

References

1. Qiao, Y.; Fring, L.D.; Pallaka, M.R.; Simmons, K.L. A review of the fabrication methods and mechanical behavior of continuous thermoplastic polymer fiber–thermoplastic polymer matrix composites. *Polym. Compos.* **2023**, *44*, 694–733. [CrossRef]
2. Das, S.C.; Paul, D.; Grammatikos, S.A.; Siddiquee, M.A.; Papatzani, S.; Koralli, P.; Islam, J.M.; Khan, M.A.; Shauddin, S.; Khan, R.A.; et al. Effect of stacking sequence on the performance of hybrid natural/synthetic fiber reinforced polymer composite laminates. *Compos. Struct.* **2021**, *276*, 114525. [CrossRef]
3. Taha, M.M.R.; Genedy, M.; Ohama, Y. 17—Polymer Concrete. In *Woodhead Publishing Series in Civil and Structural Engineering*, *Developments in the Formulation and Reinforcement of Concrete*, 2nd ed.; Mindess, S., Ed.; Woodhead Publishing: Cambridge, UK, 2019; pp. 391–408, ISBN 9780081026168. [CrossRef]
4. Zhang, X.; Du, M.; Fang, H.; Shi, M.; Zhang, C.; Wang, F. Polymer-modified cement mortars: Their enhanced properties, applications, prospects, and challenges. *Constr. Build. Mater.* **2021**, *299*, 124290. [CrossRef]
5. Beersaerts, G.; Ascensão, G.; Pontikes, Y. Modifying the pore size distribution in Fe-rich inorganic polymer mortars: An effective shrinkage mitigation strategy. *Cem. Concr. Res.* **2021**, *141*, 106330. [CrossRef]

6. Palamarchuk, A.; Yudaev, P.; Chistyakov, E. Polymer Concretes Based on Various Resins: Modern Research and Modeling of Mechanical Properties. *J. Compos. Sci.* **2024**, *8*, 503. [CrossRef]
7. Li, X.; Gu, J.; Xu, Y.; Li, S.; Zhang, R. Review of Component Materials and Diverse Applications of Polymer Concrete. *Materials* **2025**, *18*, 2745. [CrossRef] [PubMed]
8. Ramana, M.V.; Thyla, P.R.; Mahendrakumar, N.; Praveena, K. Selection of resin and aggregates for particulate polymer concrete machine tool structures—A review. *Mater. Today Proc.* **2021**, *46*, 8621–8628. [CrossRef]
9. Ferdous, W.; Manalo, A.; Wong, H.S.; Abousnina, R.; Ajarmeh, O.S.A.; Zhuge, Y.; Schubel, P. Optimal design for epoxy polymer concrete based on mechanical properties and durability aspects. *Constr. Build. Mater.* **2020**, *232*, 117229. [CrossRef]
10. Jafari, K.; Tabatabaeian, M.; Joshaghani, A.; Ozbakkaloglu, T. Optimizing the mixture design of polymer concrete: An experimental investigation. *Constr. Build. Mater.* **2018**, *167*, 185–196. [CrossRef]
11. Rajak, D.K.; Wagh, P.H.; Linul, E. Manufacturing Technologies of Carbon/Glass Fiber-Reinforced Polymer Composites and Their Properties: A Review. *Polymers* **2021**, *13*, 3721. [CrossRef] [PubMed]
12. Karahan, M.; Abbas, A.; Hussain, M. Commingled synthetic and natural fibers preforms reinforced composites: A simultaneous comparison of mechanical properties. *Polym. Compos.* **2025**, *46*, 10793–10804. [CrossRef]
13. Niaki, M.H.; Fereidoon, A.; Ahangari, M.G. Experimental study on the mechanical and thermal properties of basalt fiber and nanoclay reinforced polymer concrete. *Compos. Struct.* **2018**, *191*, 231–238. [CrossRef]
14. Huang, H.; Pang, H.; Huang, J.; Zhao, H.; Liao, B. Synthesis and characterization of ground glass fiber reinforced polyurethane-based polymer concrete as a cementitious runway repair material. *Constr. Build. Mater.* **2020**, *242*, 117221. [CrossRef]
15. McKeen, L.W. 12—Effect of Radiation on the Properties of Laminates and Composites. In *Plastics Design Library, The Effect of Radiation on Properties of Polymers*; McKeen, L.W., Ed.; William Andrew Publishing: Norwich, NY, USA, 2020; pp. 393–408. [CrossRef]
16. McKeen, L.W. 4—Effect of Radiation on the Properties of Polyester Polymers. In *Plastics Design Library, The Effect of Radiation on Properties of Polymers*; McKeen, L.W., Ed.; William Andrew Publishing: Norwich, NY, USA, 2020; pp. 93–128. [CrossRef]
17. Belkahla, N.; Teyssedre, G.; Saidi-Amroun, N.; Mouaci, S.; Saidi, M. Evaluating PET and PEN under gamma irradiation: Insights into material stability. *Radiat. Phys. Chem.* **2025**, *236*, 112912. [CrossRef]
18. Prajapati, S.; Gogoi, R.; Tyagi, V.K.; Talwar, M.; Kumar, M.; Chaudhari, C.V. Effect of gamma irradiation on shape memory, thermal and mechanical properties of polycaprolactone. *Radiat. Phys. Chem.* **2023**, *204*, 110671. [CrossRef]
19. Yi-Yang, P.; Shruti, S.; Ravin, N. Chapter 5—Modification of Polymers. In *Polymer Science and Nanotechnology*; Narain, R., Ed.; Elsevier: Amsterdam, The Netherlands, 2020; pp. 95–104. [CrossRef]
20. Rao, V.; Weimin, Y. 14—Radiation processing of Polymers. In *Advances in Polymer Processing*; Thomas, S., Ed.; Woodhead Publishing: Cambridge, UK, 2009; pp. 402–437. [CrossRef]
21. Ferry, M.; Ngono-Ravache, Y.; Aymes-Chodur, C.; Clochard, M.C.; Coqueret, X.; Cortella, L.; Pellizzi, E.; Rouif, S.; Esnouf, S. Ionizing Radiation Effects in Polymers. In *Reference Module in Materials Science and Materials Engineering*; Elsevier: Amsterdam, The Netherlands, 2016. [CrossRef]
22. Krieguer, B.; Marque, S.R.A.; Girard, F.; Dupuy, N.; Ludwig, N.; Kuntz, F.; Dorey, S. Investigation of X-Rays, e-Beam, and Gamma Irradiation on Chemical, Thermal, and Mechanical Properties of Polypropylene-Derivatives, Macromol. *Chem. Phys.* **2025**, *226*, e00130. [CrossRef]
23. More, C.V.; Alsayed, Z.; Badawi, M.S.; Thabet, A.A.; Pawar, P.P. Polymeric composite materials for radiation shielding: A review. *Environ. Chem. Lett.* **2021**, *19*, 2057–2090. [CrossRef] [PubMed]
24. da Silva, A.O.; de Castro Monsores, K.G.; de Sant, A.O.S.; Weber, R.P.; Monteiro, S.N.; de Carvalho Vital, H. Influence of gamma and ultraviolet radiation on the mechanical behavior of a hybrid polyester composite reinforced with curaua mat and aramid fabric. *J. Mater. Res. Technol.* **2020**, *9*, 394–403. [CrossRef]
25. Motaleb, K.Z.M.A.; Milašius, R.; Ahad, A. Influence of Gamma Radiation on Mechanical Properties of Jute Fabric-Reinforced Polymer Composites. *Fibers* **2020**, *8*, 58. [CrossRef]
26. Abdel-Hakim, A.; Awad, E.H.; El-Nemr, K.F.; El-Basheer, T.M. Impact of gamma radiation and multi-walled carbon nanotubes on the mechanical and acoustical properties of reinforced sisal fiber/polyester resin composites. *Radiat. Phys. Chem.* **2021**, *189*, 109768. [CrossRef]
27. Zaki, A. Preparation of polyester/gypsum/composite using gamma radiation, and its radiation stability. *Radiat. Phys. Chem.* **2005**, *73*, 183–187. [CrossRef]
28. Bansal, N.; Arora, S. Exploring the impact of gamma rays and electron beam irradiation on physico-mechanical properties of polymers & polymer composites: A comprehensive review. *Nucl. Instrum. Methods Phys. Res. B* **2024**, *549*, 165297. [CrossRef]
29. Elsawy, M.A.; Fekry, M.; Sayed, A.M.; Maziad, N.A.; Saad, G.R. Physico-chemical Characteristics of Biodegradable Poly(lactic acid) and Poly(lactic acid)/Chitosan Nano-Composites Under the Influence of Gamma Irradiation. *J. Polym. Environ.* **2023**, *31*, 2705–2714. [CrossRef]

30. Nabiyev, A.; Ivankov, O.; Azhibekov, A.; Elmekawy, A.; Popov, E.; Samadov, S.; Trung, N.; Mutali, A.; Sidorin, A.; Orlov, O.; et al. High-dose gamma irradiation effects on HDPE/SiO_2 nanocomposite films: Structure, crystallinity, defects, radiation endurance, dispersion, and interfacial behavior. *Polym. Degrad. Stab.* **2026**, *245*, 111851. [CrossRef]
31. Da Costa, F.A.T.; Dufresne, A.; Parra, D.F. Effective compatibilization of poly(L-lactic acid)/poly(butylene adipate-co-terephthalate) blends via low-dose gamma irradiation. *Int. J. Biol. Macromol.* **2026**, *361*, 152013. [CrossRef] [PubMed]
32. Saiyad, M.; Devashrayee, N.M.; Mewada, R.K. The influence of stabilisers on resistance to gamma radiation for epoxy based polymeric composite material. *Compos. Part B Eng.* **2014**, *57*, 71–79. [CrossRef]
33. Chen, K.; Zhao, X.; Zhang, F.; Wu, X.; Huang, W.; Liu, W.; Wang, X. Influence of Gamma Irradiation on the Molecular Dynamics and Mechanical Properties of Epoxy Resin. *Polym. Degrad. Stab.* **2019**, *168*, 108940. [CrossRef]
34. Szajerski, P.; Celinska, J.; Gasiorowski, A.; Anyszka, R.; Walendziak, R.; Lewandowski, M. Radiation induced strength enhancement of sulfur polymer concrete composites based on waste and residue fillers. *J. Clean. Prod.* **2020**, *271*, 122563. [CrossRef]
35. Chen, R.S.; Ghani, M.H.A.; Ahmad, S.; Tarawneh, M.A.; Gan, S. Tensile, thermal degradation and water diffusion behaviour of gamma-radiation induced recycled polymer blend/rice husk composites: Experimental and statistical analysis. *Compos. Sci. Technol.* **2021**, *207*, 108748. [CrossRef]
36. Magida, M.M.; Ibrahim, S.M.; Elnahas, H.H. Effect of gamma radiation on the characterization of chitosan/natural rubber latex polymer blends. *Int. J. Polym. Anal. Charact.* **2020**, *25*, 565–580. [CrossRef]
37. Sirin, M.; Zeybek, M.S.; Sirin, K.; Abali, Y. Effect of gamma irradiation on the thermal and mechanical behaviour of polypropylene and polyethylene blends. *Radiat. Phys. Chem.* **2022**, *194*, 110034. [CrossRef]
38. Xiao, Y.; Zhang, F.; Wei, R.; Qin, D.; Tang, Z.; Bao, Y.; Cai, Z. Influence of γ-irradiation dose on the mechanical and tribological properties of fluoroelastomer. *Polym. Eng. Sci.* **2024**, *64*, 5186–5197. [CrossRef]
39. Mahboubizadeh, S.; Sadeq, A.; Arzaqi, Z.; Ashkani, O.; Samadoghli, M. Advancements in fiber-reinforced polymer (FRP) composites: An extensive review. *Discov. Mater.* **2024**, *4*, 22. [CrossRef]
40. Goda, I.; Padayodi, E.; Raoelison, R.N. Enhancing fiber/matrix interface adhesion in polymer composites: Mechanical characterization methods and progress in interface modification. *J. Compos. Mater.* **2024**, *58*, 3077–3110. [CrossRef]
41. Blazy, J.; Drobiec, L.; Wolka, P. Flexural Tensile Strength of Concrete with Synthetic Fibers. *Materials* **2021**, *14*, 4428. [CrossRef] [PubMed]
42. Shahriar, M.F.; Rahman, R.; Kamal, T. An overview of the application of recycled textile fibers in structural concrete. *Discov. Concr. Cem.* **2025**, *1*, 29. [CrossRef]
43. Nouri, N.; Hosseinpoor, M.; Yahia, A.; Khayat, K.H. Coupled effect of fiber and granular skeleton characteristics on packing density of fiber-aggregate mixtures. *Constr. Build. Mater.* **2022**, *342*, 127932. [CrossRef]
44. Rajak, D.K.; Wagh, P.H.; Linul, E. A Review on Synthetic Fibers for Polymer Matrix Composites: Performance, Failure Modes and Applications. *Materials* **2022**, *15*, 4790. [CrossRef] [PubMed]
45. Sharma, H.; Kumar, A.; Rana, S.; Sahoo, N.G.; Jamil, M.; Kumar, R.; Sharma, S.; Li, C.; Kumar, A.; Eldin, S.M.; et al. Critical review on advancements on the fiber-reinforced composites: Role of fiber/matrix modification on the performance of the fibrous composites. *J. Mater. Res. Technol.* **2023**, *26*, 2975–3002. [CrossRef]
46. Hidayat, E.J.; Kundari, N.A.; Saputra, A. Waste tire granular modification using gamma radiation as concrete aggregate. *Rekayasa Hijau* **2022**, *6*, 229–237. [CrossRef]
47. Kiss, L.; Simon, D.A.; Barany, T.; Meszaros, L. Synergistic effects of gamma pre-irradiation and additional vulcanizing agent in case of ground tire rubber containing vulcanizates. *Radiat. Phys. Chem.* **2022**, *201*, 110414. [CrossRef]
48. Alhazmi, H.; Shah, S.A.R.; Anwar, M.K.; Raza, A.; Ullah, M.K.; Iqbal, F. Utilization of polymer concrete composites for a circular economy: A comparative review for assessment of recycling and waste utilization. *Polymers* **2021**, *13*, 2135. [CrossRef] [PubMed]
49. Mohammed, M.; Oleiwi, J.K.; Mohammed, A.M.; Jawad, A.J.M.; Osman, A.F.; Adam, T.; Betar, B.O.; Gopinath, S.C.; Dahham, O.S.; Jaafar, M. Comprehensive insights on mechanical attributes of natural-synthetic fibres in polymer composites. *J. Mater. Res. Technol.* **2023**, *25*, 4960–4988. [CrossRef]
50. Penner, E.; Caylak, I.; Mahnken, R. Experimental Investigations of Carbon Fiber Reinforced Polymer Composites and Their Constituents to Determine Their Elastic Material Properties and Complementary Inhomogeneous Experiments with Local Strain Considerations. *Fibers Polym.* **2023**, *24*, 157–178. [CrossRef]
51. Kishi, H.; Arimura, K.; Idesaki, A.; Kakibe, T.; Matsuda, S. Effect of γ-ray irradiation on epoxy network polymers with different curing agents. *Polym. Adv. Technol.* **2022**, *33*, 3740–3749. [CrossRef]
52. Jamalzadeh, M.; Sobkowicz, M.J. Review of the effects of irradiation treatments on poly(ethylene terephthalate). *Polym. Degrad. Stab.* **2022**, *206*, 110191. [CrossRef]
53. Chayoukhi, S.; Abid, M.; Gassoumi, B.; Mejri, A.; Boukhachem, A.; Amlouk, M. Experimental and numerical studies of the mechanical properties of nitrile-butadiene rubber exposed to gamma radiation. *Radiat. Phys. Chem.* **2023**, *208*, 110925. [CrossRef]

54. Fatoni, N.; Ferianto, M.D.; Rivaldi, M.R.; Welerubun, I.Y.P. The effect of gamma irradiation on quality of composite from bagasse, bamboo, and polypropylene coated resin. *Proc. Intl. Conf. Sci. Eng.* **2021**, *4*, 150–154.
55. Bansal, N.; Jagdeva, G.; Lal, S.; Arora, S. Synergistic effects of gamma irradiation and Delonix regia pods bio-waste on the physico-mechanical properties of recycled-polypropylene composites: A design of experiment approach. *Radiat. Phys. Chem.* **2024**, *214*, 111293. [CrossRef]

Disclaimer/Publisher's Note: The statements, opinions and data contained in all publications are solely those of the individual author(s) and contributor(s) and not of MDPI and/or the editor(s). MDPI and/or the editor(s) disclaim responsibility for any injury to people or property resulting from any ideas, methods, instructions or products referred to in the content.